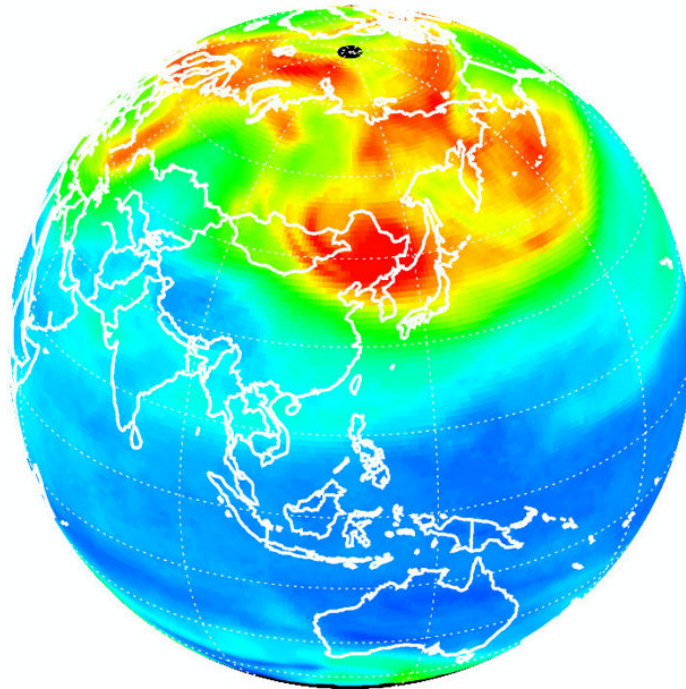


Version 3 Level 2 EPIC total ozone: data quality and description document



December 9, 2020

Natalya Kramarova¹, Liang-Kang Huang^{1,2}, Jerald R. Ziemke^{1,3}, Jay Herman^{1,4}

¹NASA Goddard Space Flight Center, ²Science Systems and Applications Incorporated, ³Morgan State University,
⁴University of Maryland Baltimore County

Table of contents:

1. SPACECRAFT AND INSTRUMENT.....	3
2. UV CHANNEL CALIBRATIONS	4
<u>3.</u> TOTAL OZONE RETRIEVAL ALGORITHM	8
4. TOTAL OZONE LEVEL 2 OUTPUT FILE.....	12
5. VERSION 3 TOTAL OZONE: DATA QUALITY AND SCREENING	14
REFERENCES:	19

This document is created in support of the DSCOVR-2017 Science Team proposal *“Improving total and tropospheric ozone column products from EPIC on DSCOVR for studying regional scale transport”*.

1. Spacecraft and Instrument

The DSCOVR (Deep Space Climate Observatory) spacecraft carrying the EPIC (Earth Polychromatic Imaging Camera) instrument was successfully launched on February 11, 2015 to the Earth-Sun Lagrange-1 point (L-1) arriving in mid-June 2015 (1.5×10^6 km from Earth) shortly before the first monochromatic image was received back on Earth. EPIC, one of instruments onboard of DSCOVR, permits measurements of ozone, aerosol amounts, and cloud reflectivity, using a Couple Charge Device (CCD) detector with 2048 by 2048 pixels to obtain Earth images with four ultraviolet channels (317.5, 325, 340 and 388 nm) in addition to four visible channels (443, 551, 680 and 687.75 nm) and two near-IR channels (764 and 779.5 nm). The EPIC instrument consists of a 30 cm aperture Cassegrain telescope and a multi-element field-lens group capable focusing light on the UV sensitive CCD detector after sequentially passing through ten narrow-band filters mounted in two moveable filter wheels and an exposure control rotating shutter. The 10 filter transmission functions for each EPIC channel are shown in Figure 1. Of these, the UV filters have bandpass with full widths at half maximum 1.0, 1.0, 2.7 and 2.6 nm, respectively. Only the blue 443 nm channel is downlinked at full resolution to help with resolving cloud cover and improving Earth color images. The image sampling resolution of a single pixel is about 8×8 km², but after accounting for the effect of the optical point-spread function, the effective 443 nm channel resolution is about 10 km. For the other channels, four (2x2) individual pixels are averaged onboard of spacecraft to yield an effective 1024×1024 pixel image corresponding to an 18×18 km² resolution at the observed center of the Earth's sunlit disk. The effective spatial resolution decreases as the secant of the angle between EPIC's sub-earth point and the normal to the earth's surface (i.e., at an angle of 60° , the resolution would be 36×36 km²).

A regular earth measurement sequence includes 10 images starting with 443 nm followed by 551 nm, 688 nm, 680 nm, 764 nm, 780 nm, 388 nm, 340 nm, 325 nm and 317 nm in 7 minutes. Except for 443 nm, all other 9 channels are roughly 27 seconds apart from each other. The exposure times for each wavelength were adjusted in-flight to achieve ~ 80% fill of CCD's electron wells over the brightest scenes to avoid leaking from one pixel to another (blooming). Exposure times range from 1 second at 317.5 nm to 25 milliseconds at 551 nm, and have not changed during the life of the mission. Limited by coverage of ground stations for transmission bandwidth of data from the satellite, EPIC can take hourly earth measurements during the northern summer. A minimum of 13 measurements per day happens during the northern winter. Therefore, EPIC can provide synoptic global measurements from sunrise to sunset every hour or every other hour.

2. UV Channel Calibrations

Before the raw EPIC data (counts per second) can be used, a number of pre-processing steps must be accomplished. The major steps are 1) measuring and subtracting the dark current signal, 2) “flat-fielding” the CCD so that the sensitivity differences between all four million pixels are determined and corrected, 3) correcting for stray-light effects to account for light that should be going to a particular pixel, but instead is scattered to different pixels, and 4) determining the radiometric calibration for each wavelength channel in terms of EPIC counts/second to be converted to earth normalized radiances. The earth upwelling radiance I_M ($W/(m^2 nm sr)$) at the top of the atmosphere (TOA) is related to the normalized radiance, or called Earth’s albedo A_M in [sr^{-1}], by

$$A_M = \frac{I_M}{S_M/D_E^2} \quad (1)$$

for wavelength bands M=1 to 4, S_M is the weighted wavelength average of the incident solar irradiance ($W/(m^2 nm)$) for band M at 1 AU and D_E is the sun-earth distance in AU (astronomical units).

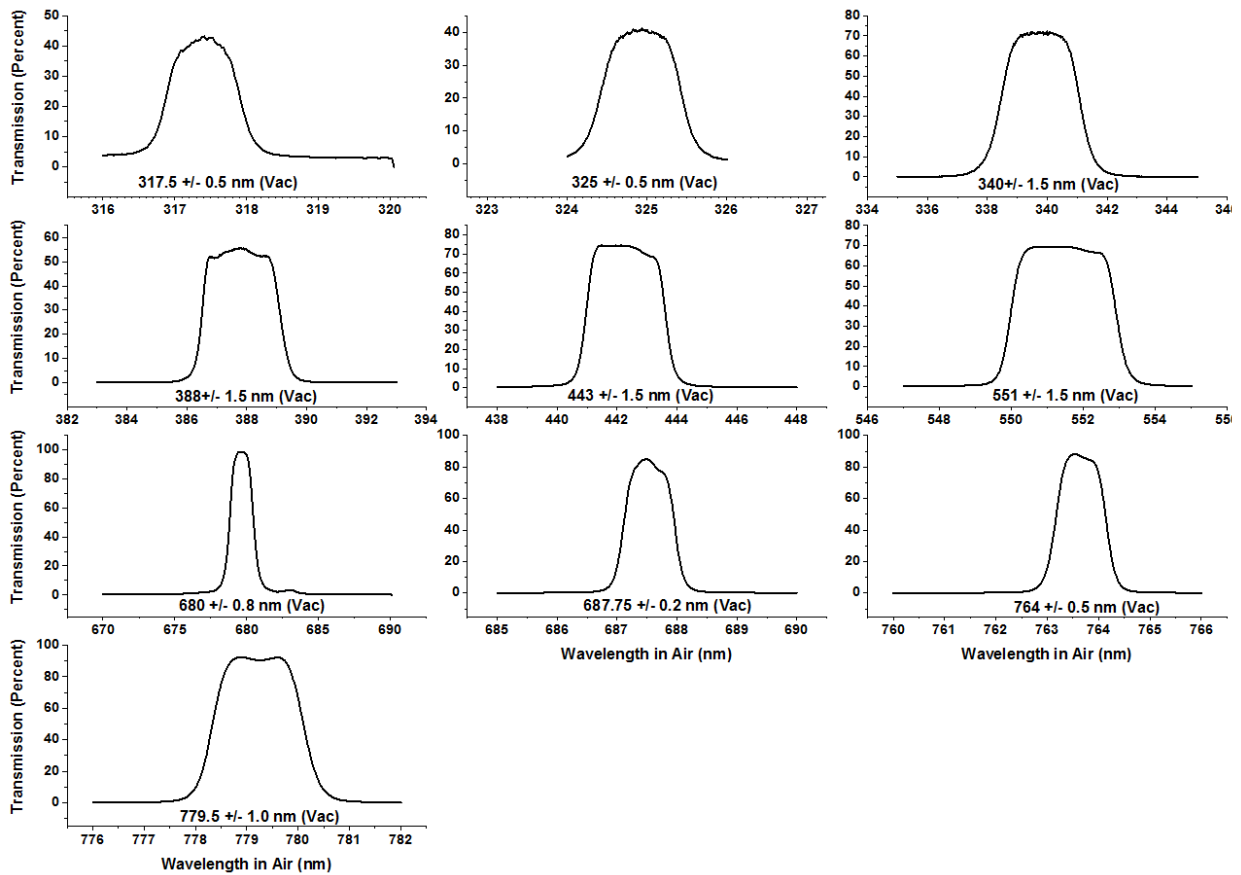


Figure 1. EPIC’s spectral filter transmission (percent) for the 10 wavelengths. The central band wavelength and full width at half maximum (FWHM) in [nm] are indicated for each channel.

Since EPIC does not measure solar irradiance, we use the high-resolution solar irradiance spectrum, $S(\lambda)$ [Dobber et al., 2008], as a reference solar spectrum. The reference spectrum is convolved with EPIC's filter transmission functions $T_M(\lambda)$ (see Figure 1) to obtain the weighted solar irradiance S_M for each EPIC's channel at solar-earth distance of 1 astronomical unit,

$$S_M = \int T_M(\lambda)S(\lambda)d\lambda / \int T_M(\lambda)d\lambda \quad (\text{Wm}^{-2}\text{nm}^{-1}) \quad (2)$$

In-flight radiometric calibration is accomplished by comparison with albedo values measured by current well-calibrated Low Earth Orbiting (LEO) satellite instruments, Suomi-NPP/OMPS and Aura/OMI, over scenes where observational time and angles match to those from EPIC. For albedo measurements, OMPS has a calibration accuracy of 2%, while its wavelength dependence (precision) in the calibration is estimated to be better than 1% [Seftor et al., 2014]. OMPS Nadir Mapper (NM) on Suomi-NPP has a 50x50 km² footprint in its normal operational mode with 36 cross-track views ($\pm 55^\circ$ satellite view zenith angle, ± 1300 km or about $\pm 12^\circ$ equatorial longitude). In the comparison, about 7x7 EPIC pixels that filled in a selected OMPS NM footprint are averaged. OMPS NM has a spectral resolution of 1 nm, which is close to EPIC's 317.5 nm and 325 nm channels FWHM, but narrower than the EPIC's 340 nm and 388 nm channels. To perform in-flight calibration, OMPS albedo spectra were either interpolated (for 317.5 and 325 nm channels) or convolved (at 340 and 388 nm) with each EPIC filter transmission function T_M (Fig. 1). In the albedo spectra $A_M(\lambda)$ Fraunhofer solar line structures are cancelled out (Eq. 1), therefore interpolation and convolution of $A_M(\lambda)$ have better accuracy than direct convolution and interpolation of the radiance spectra $I_M(\lambda)$. OMI on Aura has 13 km x 24 km spatial resolution and about $\pm 56^\circ$ cross-track views (± 1300 km or $\pm 13^\circ$ equatorial longitude) with a spectral resolution of 0.42 nm. To match measurements with DSCOVR, OMI's albedo spectra were convoluted with EPIC's $T_M(\lambda)$. Then, the results in every two adjacent cross-track views and four consecutive along-track scans for OMI are combined to form 50x50 km² footprints for comparison with EPIC.

EPIC raw counts per second inside each coincident footprint are preprocessed after the steps stated in a previous paragraph. Then, the counts/second average and variance in each coincident footprint are computed to obtain the EPIC albedo calibration coefficients K_M (Eq. 3):

$$K_M = \frac{A_M(\text{OMPS})\{\alpha_M(\text{EPIC})/\alpha_M(\text{OMPS})\}}{C_M(\text{EPIC})D_E^2} \quad (3)$$

where M is the EPIC channel number for UV wavelengths, M=1,2,3,4. $A_M(\text{OMPS})$ is OMPS albedo measurement at the EPIC wavelength M, $\alpha_M(\text{EPIC})$ and $\alpha_M(\text{OMPS})$ are computed albedo values for EPIC and OMPS coincident observations, $C_M(\text{EPIC})$ is the average EPIC count rate over the pixels matching OMPS, and D_E is the sun-earth distance in AU.

$$\alpha_M = \int \alpha(\lambda)S(\lambda)T_M(\lambda)d\lambda / \int S(\lambda)T_M(\lambda)d\lambda \quad (4)$$

where $\alpha(\lambda)$ is the computed high-resolution normalized radiance spectrum, $S(\lambda)$ is the referenced high-resolution solar irradiance spectrum, $T_M(\lambda)$ is either the EPIC's filter transmission profile or the OMPS NM spectrometer's bandpass.

Misalignment between EPIC and OMPS or OMI footprints can result in a large scene noise unless uniform scenes are selected and less uniform scenes discarded. This is achieved by weighting each coincidence data point with the reciprocal of the percent EPIC counts/second variance inside the coincident footprint. All of the coincident points between LEO satellites and EPIC observations occur within $\pm 40^\circ$ of the Earth’s equator. Selected LEO footprints have viewing angles nearly identical to EPIC’s (within 1° in backscatter angle and 2° degrees in solar zenith angle). EPIC’s backscatter angles vary with latitude and longitude by less than 0.25° , since the angular diameter of the earth varies from 0.45° to 0.53° depending on the location of DSCOVR in its orbit (an irregular Lissajous orbit perturbed by the Earth’s moon). The orbit varies from 4° to 15° away from the Earth-Sun line. These small differences in observing geometry are corrected in the atmospheric radiative transfer model calculations $\alpha(\lambda)$ (Eq. 4), resulting in corrections to K_M (Eq. 3) less than 2%.

All of the coincidence points with LEO satellite instruments were measured using the central area of the EPIC CCD within 600 pixels of its center. There are about 60000 coincidence data points accumulated by the end of August 2020. Because of the large number of data points, statistical averaging errors are small. An atmospheric radiative transfer model, RTM, takes total column ozone for construction of a priori ozone profile and surface reflectivity from LEO retrievals to obtain both $\alpha_M(\text{EPIC})$ and $\alpha_M(\text{LEO})$. Although uncertainties in the RTM can propagate into the computed albedos, the resulting uncertainties in $\alpha_M(\text{EPIC})$ and $\alpha_M(\text{LEO})$ are approximately identical and canceled out in Eq. 3. The resulting EPIC albedo calibration uncertainty is mostly inherited from the OMPS albedo calibration uncertainty, which has an accuracy of 2% and a precision of 1% in relative (wavelength dependent) values. For the UV channels, the calibration factors K_M are not constants, but are slowly increasing functions of time. Table 1 shows the reference values of K_M multiplied by π on January 1, 2016. The time dependent multiplier is shown in Figure 2, which is normalized to 1 at $t=2016$. Using Table 1 and Figure 2, EPIC measured albedo is derived as:

$$A_M(\text{EPIC}) = K_M C_M(\text{EPIC}) D_E^2 \tag{5}$$

Table 1. EPIC albedo calibration coefficients $K_M(\lambda, t=2016)$ multiplied by π in $[\text{CountRate} * (\text{mW}/\text{m}^2/\text{nm})]$ at 4 UV channels and solar irradiances S_M convolved with EPIC transmission function.

Table 1 πK_M on 1 January 2016			Irradiance at 1 AU
M	λ (nm)	πK_{M0}	$S_M(\text{mW}/\text{m}^2/\text{nm})$
1	317.478	1.216E-04	819.0
2	325.035	1.111E-04	807.7
3	339.858	1.975E-05	995.8
4	387.923	2.685E-05	1003.0

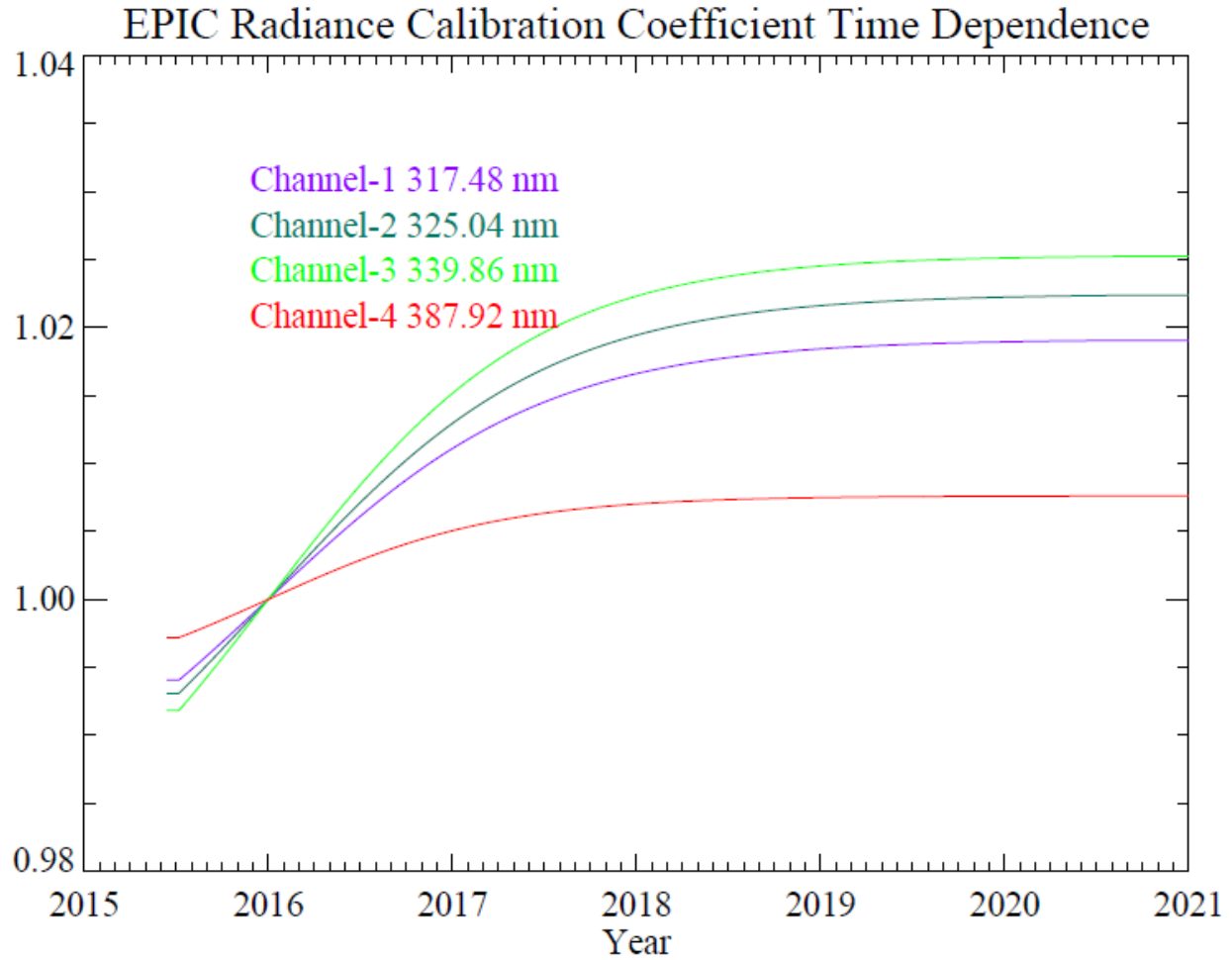


Figure 2. The time dependence factors of EPIC radiance calibration coefficients K_M . The calibration coefficients at Year 2016.0 are given in Table 1. The data from the coincidence comparison with SNPP OMPS NM (updated to August 31, 2020) are fitted with hyperbolic tangent functions and the fitted curves are extrapolated for EPIC's operational data processing.

3. Total Ozone Retrieval Algorithm

Once the calibration factors are applied to EPIC's measured counts/second, the resulted albedo measurements can be combined to retrieve total column ozone (TCO), Lambert Equivalent Reflectivity (LER), and aerosol index (AI). In order to make the retrieved ozone values consistent with SNPP NM total ozone, the constant N-value adjustments are added to the measured EPIC N-values (given by Eq. 5). In this version 3 release, the constant N-value adjustments are determined from zonal mean comparisons of EPIC and OMPS measurements in equatorial latitude band (-2.5°S to +2.5°N) at local solar hours between 12:30 pm and 2:30 pm. Results from four weeks around Equinoxes and Solstices in 2017 are used to determine the constant N-Value adjustments, often called as the soft calibration. This N-value adjustment not only provides correction to possible offsets in the EPIC's albedo calibration derived in the section 2, but also provides adjustments to various differences between EPIC's and OMPS's ozone retrieval algorithms.

The EPIC version 3 ozone retrieval algorithm adopts many components of the Version 8 TOMS algorithm [Rodriguez et al., 2003; Bhartia and Wellemeyer, 2002]. The TOMRAD radiative transfer model is used to simulate EPIC sun normalized radiances (or albedos) at the top of the atmosphere (TOA). TOMRAD has a spherical geometry correction for large solar zenith angles (SZAs) and satellite look angles (SLAs) [Caudill et al., 1997]. Spectrally resolved ozone absorption cross sections are from Brion et al. [1998]; Daumont et al. [1992]; and Malicet et al. [1995]. To speed up the ozone retrieval algorithm, calculated albedos are compiled in a look-up table as a function of ozone profiles and solar-view angles. The TOA radiances are calculated for 26 climatological ozone profiles that cover a broad range of total column values between 125 DU and 575 DU [McPeters et al., 1996], using a climatological mean mid-latitude temperature profile. Climatological ozone profiles are defined at 11 Umkehr layers, with pressure at the bottom of each layer defined as $P_{\text{bottom}}(i) = 1013.25 * 0.5^{(i-1)}$, where i is a layer index 1, 2, 3, ..., 11. To simulated EPIC observation geometry, TOMRAD calculations are done for a range of SZA (0°, 30°, 45°, 60°, 70°, 77°, 81°, 84°, 86°, and 88°) and SLA (0°, 15°, 30°, 45°, 60°, 70°, 77°, 81°, 84°, 86°, and 88°), and for four terrain/cloud top pressure values (1013.25 hPa, 709.25 hPa, 405.3 hPa, and 202.65 hPa). The calculated high resolution spectra for TOA radiances are convoluted with both EPIC UV filter's transmission functions and the reference solar spectra. In addition, TOA directional albedo values are computed by perturbing layer ozone values for each of the 26 ozone profiles in order to determine the albedo sensitivity to ozone profile changes. The retrieval code uses Lagrange polynomials to interpolate the tabulated TOMRAD results to observed EPIC's solar/view zenith angles.

The TOA albedo represents the sum of atmospheric backscattering light and light reflected from the surface:

$$\alpha_{\lambda}(p) = \alpha_{0\lambda}(p) + \frac{t_{\lambda}(p)R}{1 - S_{b\lambda}(p)R} \quad (6)$$

where the first term, $\alpha_{0\lambda}(p)$, represents TOA albedo for nonreflecting surface (with $R=0$), $t_{\lambda}(p)$ is a fraction of direct and diffused light reaching the surface and emerging at TOA, R is the surface reflectivity, $S_{b\lambda}(p)$ is a fraction of light reflected from the surface and scattered back to the surface by the atmosphere, and p is the terrain/cloud top pressure and λ is the centroid wavelength of the filter's transmission function. The second term in eq (6) is related to the contribution from the reflecting surface with the reflectivity value R .

The retrieval algorithm uses the logarithm of albedo values called N-values defined as:

$$N_{\lambda} = -100 \log_{10}(\alpha_{\lambda}) \quad (7)$$

For the computed albedo with Eqs. 4 and 6, and

$$N_M = -100 \log_{10}(A_M) \quad (8)$$

for the measured albedo where A_M is obtained with Eq 5. In addition to calculating TOA albedos, the tabulated albedo values are also used to estimate sensitivities of TOA albedos to changes in total column ozone $\frac{\partial N_{\lambda_i}}{\partial \Omega}$, reflectivity $\frac{\partial N_{\lambda_i}}{\partial R}$, ozone profile $\frac{\partial N_{\lambda_i}}{\partial X_i}$, and temperature profile $\frac{\partial N_{\lambda_i}}{\partial T_i}$.

EPIC ozone retrieval algorithm uses the 388 nm channel to estimate the surface reflectivity. The minimum terrain surface reflectivity is defined by the OMI-based climatology of terrain minimum surface reflectivity, which changes with season and geolocation [Kleipool et al., 2008]. The partial cloud algorithm, developed for the TOMS Version 7 [McPeters, et. al 1996], is used to determine cloud fraction and to combine radiances scattered and reflected from the terrain surface and from clouds.

In the previous version, the cloud pressure was determined using the OMI UV radiative cloud effective pressure height climatology [Vassilkov et al., 2008]. Since EPIC measures the oxygen A-band absorption and retrieves the real-time cloud height [Yang et al., 2019], this product is now used in version 3 EPIC ozone algorithm. Wherever the A-band cloud pressure height is not available, the ozone retrieval algorithm uses cloud effective pressure from the OMI-based climatology.

In the presence of clouds, the partial cloud algorithm computes two albedo values: one value α_{λ_g} for climatological minimum surface reflectivity at terrain pressure, and another albedo value α_{λ_c} for reflectivity $R=0.8$ at the cloud height. The cloud fraction is determined as:

$$f_c = \frac{A_{M_0} - \alpha_{\lambda_0 g}}{\alpha_{\lambda_0 c} - \alpha_{\lambda_0 g}} \quad (9)$$

where λ_0 and M_0 corresponds to EPIC's 388 nm channel for calculated and measured albedo, respectively, and f_c is limited to values between 0 and 1. The partial cloud reflectivity (between clear sky and fully clouded sky $0 < f_c < 1$) is determined as:

$$R(0 < f_c < 1) = R_{gmin}(1 - f_c) + R_{cmin}f_c \quad (10)$$

where R_{gmin} is the climatological surface minimum reflectivity, and $R_{cmin}=0.8$ is the assumed cloud minimum reflectivity. For partially cloudy scenes, the algorithm assumes that the TOA albedo is a linear combination of the clear sky albedo and the albedo from the cloud surface:

$$\alpha_{\lambda}(0 < f_c < 1) = \alpha_{\lambda g}(1 - f_c) + \alpha_{\lambda c}f_c \quad (11)$$

In cases of clear sky ($f_c \leq 0$ with Eq 9) or fully cloudiness ($f_c \geq 1$ with Eq 9), the algorithm computes the reflectivity at 388 nm to force the computed α_{λ} in Eq. 6 to be equal to the measured A_M :

$$R = \frac{A_{M_0} - \alpha_{0\lambda_0}}{t_{\lambda_0} + S_b \lambda_0 (A_{M_0} - \alpha_{0\lambda_0})} \quad (12)$$

where α_0 , t and S_b are computed either at the terrain pressure or cloud pressure.

In the current version 3, the ozone retrieval algorithm accounts for ozone and temperature profile seasonal and latitudinal variations using seasonal a priori ozone profile climatology [McPeters and Labow, 2012] and temperature climatology. The calculated TOA N-values are adjusted for differences between the a priori ozone (or temperature) profiles and the standard climatological profiles used for computing

the lookup tables. That profile differences are converted in changes in N-values using linear approximation and calculated sensitivities $\frac{\partial N_{\lambda_i}}{\partial x_i}$ (or $\frac{\partial N_{\lambda_i}}{\partial T_i}$).

The important assumption in the EPIC's ozone retrieval algorithm is that the surface reflectivity changes linearly with wavelength [*Herman et al., 2018*]:

$$R_{\lambda} = R_{\lambda_0} + b(\lambda - \lambda_0) \quad (13)$$

where λ is a given wavelength, and λ_0 is a reference wavelength 388 nm. Note, that in Versions 7 and 8 of TOMS total ozone retrieval algorithms the surface reflectivity is assumed to be constant for computing TOA albedo values at different wavelengths. Though the wavelength dependence in EPIC's UV range is typically small, but it can reach several percent in some cases depending on terrain surface types. Scene reflectivity observed by satellite can also be altered by the presence of aerosols. This linear wavelength dependence of the surface reflectivity provides an effective aerosol correction, which however may not be accurate for all types of aerosols.

EPIC's retrieval algorithm uses a wavelength triplet to derive total ozone column. Two ozone absorption channels either 317.5 and 340 nm or 325 and 340 nm, depending on optical depth conditions, are combined with the 388 nm channel which has no ozone absorption. The total column ozone (TCO) Ω is derived as:

$$\Omega_n = \Omega_{n-1} + \frac{\Delta N_{\lambda_1} \frac{\partial N_{\lambda_2}}{\partial R} (\lambda_2 - \lambda_0) - \Delta N_{\lambda_2} \frac{\partial N_{\lambda_1}}{\partial R} (\lambda_1 - \lambda_0)}{\frac{\partial N_{\lambda_1}}{\partial \Omega} \frac{\partial N_{\lambda_2}}{\partial R} (\lambda_2 - \lambda_0) - \frac{\partial N_{\lambda_2}}{\partial \Omega} \frac{\partial N_{\lambda_1}}{\partial R} (\lambda_1 - \lambda_0)} \quad (14)$$

where Ω_{n-1} is TCO from previous iteration or initial estimate, λ_1 and λ_2 are the selected ozone absorption wavelengths, ΔN_{λ_i} is the N-value residuals (difference between measured and calculated albedos expressed in N-values), $\frac{\partial N_{\lambda_i}}{\partial \Omega}$ is the computed TOA albedo sensitivity with respect to the total column ozone, $\frac{\partial N_{\lambda_i}}{\partial R}$ the computed sensitivity to the surface reflectivity at wavelengths λ_1 or λ_2 . If one assumes that the sensitivity to the surface reflectivity ($\partial N_{\lambda_i} / \partial R = \text{const}$) is independent of wavelength, then the eq. 14 for the triplet algorithm falls to the Version 7 TOMS triplet equation [*Rodriguez et al., 2003*]. After each iteration the resulted ozone value Ω_n will be used to select the climatological ozone profiles in the lookup tables and re-compute TOA albedos. Several iterations are performed until the difference between the retrieved ozone column Ω_n and the ozone column derived in the previous iteration Ω_{n-1} is less than 0.5 DU.

Note that the residuals for the wavelength channels in the triplet algorithm are equal to zeros after the final iteration. The code reports residuals at 317.5, 325 and 340 nm that are computed with a wavelength independent surface reflectivity R as determined with the 388 nm channel. The code also reports the spectral slope for the reflectivity values at UV channels (coefficient b (1/nm) in Eq. 13). In cases with elevated aerosol, the spectral slope can be significant, leading to increase in reported residuals at ozone absorption wavelengths. This triplet algorithm with wavelength-dependent reflectivity R_{λ} allows to adjust both - the total ozone amount and the reflectivity at the ozone absorption wavelengths to account

for the presence of aerosol. The retrieved ozone values over aerosol area in large pyroCb events and desert storm events are consistent with those in the surrounding area without aerosol contamination. This aerosol correction mechanism would not work in cases of volcanic eruptions because of the presence of SO₂, which is not included in the RTM computation. This approach also helps to reduce errors caused by the Sun glint (in cases with low (<30°) SLA over water surface and clear sky conditions), which produces a departure from the Lambertian surface reflectivity model. This triplet algorithm with a simple linear model for surface reflectivity, implemented for EPIC, provides an effective aerosol correction mechanism that distinguishes it from the heritage algorithms.

To facilitate error analysis, Column Weighting Functions had been included in version 3 processing. UV measurements have reduced sensitivity to ozone changes in the boundary layer. CWF are aimed to help users to interpretate EPIC total ozone retrievals and indicate the weight of measurements in each layer. EPIC CWF had been calculated using eq. 4.10 from [Rodgers, 2000]:

$$A = S_a K^T (K S_a K^T + S_e)^{-1} K \quad (15)$$

where A is Averaging Kernel matrix with 11 by 11 elements, K is the matrix with ozone profile sensitivity $\frac{\partial N_\lambda}{\partial x_\lambda}$ for M EPIC UV channels used in the ozone retrievals. S_e is error covariance matrices M x M that has only diagonal elements equivalent to 1% error (or 0.43 N-value). S_a is a priori covariance matrix (11 by 11) that is defined as:

$$S_a(i, j) = 0.5 * x_a(i) * 0.5 * x_a(j) * (e)^{|i-j|/3.5} \quad (16)$$

Where x_a climatological ozone profile, and i and j layer indexes from 1 to 9. Finally, CWF are determined by summing rows of the Averaging Kernel matrix:

$$CWF(i) = \sum_{j=1}^{j=9} A(i, j) \quad (17)$$

The shape of CWF is determined by sensitivity of albedos to ozone profile changes $\frac{\partial N_\lambda}{\partial x_\lambda}$. We recommend using values of CWF in the lowest layer i=1 to determine sensitivity of EPIC total column retrievals to ozone changes in the lowest layer. However, it is important to note that we do not use the Optimal Estimation technique and therefore Averaging Kernels and Column Weighting Functions derived from Equations (15-17) should be used with caution for layers in the stratosphere (i ≥ 3).

4. Total Ozone Level 2 Output File

The retrieved ozone values and other variables for the ozone measurements are saved in HDF5 files. The filename convention is DSCOV_R_EPIC_L2_TO3_##_YYYYMMDDHHMMSS_?.h5, where ## (currently 03) is for the retrieval algorithm version number, ?? (currently 03) is for the version of input L1b, the date and timing are given in YYYY for year, MM for month, DD for day in the month, HHMMSS for hour, minute and seconds in UTC. For example, file DSCOV_R_EPIC_L2_TO3_03_20151007043937_03.h5 contains EPIC total ozone measurements on October 7, 2015, at UTC 04:39:37. The version 03 total ozone retrieval algorithm is used. The input is from version 03 EPIC L1b file. All variables included in the Level 2 Total Ozone files are defined in Table 3.

Table 3. Content of EPIC total ozone Level 2 files.

Name	Type	Dimension	Units	Description
Latitude	Real*4	2048x2048	degrees	Latitude
Longitude	Real*4	2048x2048	degrees	Longitude
SolarZenithAngle	Real*4	2048x2048	degrees	Solar Zenith Angle
SatelliteZenithAngle	Real*4	2048x2048	degrees	Satellite Zenith Angle
SolarAzimuthAngle	Real*4	2048x2048	degrees	Solar Azimuth Angle
SatelliteAzimuthAngle	Real*4	2048x2048	degrees	Satellite Azimuth Angle
TerrainPressure	Real*4	2048x2048	fraction	Terrain Pressure, normalized at 1013.25 hPa
CloudPressure	Real*4	2048x2048	fraction	Cloud Pressure, normalized at 1013.25 hPa
Ozone	Real*4	2048x2048	DU	Retrieved Column Total Ozone
RadiativeCloudFraction	Real*4	2048x2048	fraction	Radiative Cloud Fraction (range from 0 to 1)
Reflectivity	Real*4	2048x2048	Reflectivity Units RU fraction	Surface Reflectivity (range from 0 to 1)
SlopeOfReflectivity	Real*4	2048x2048	1/nm	Slope of Surface Reflectivity for the triplet
LERTerrPres	Real*4	2048x2048	fraction	Reflectivity computed with reflecting surface set at terrain pressure height
ErythemaUV	Real*4	2048x2048	w/m ²	Erythema UV irradiance
OzoneStep1	Real*4	2048x2048	DU	Column total ozone values computed with the standard climatological ozone and temperature profiles
AlgorithmFlag	Integer*2	2048x2048	Unitless	Algorithm flag 1 - 317, 340 & 388 nm triplet + A-Band cloud pressure; 2 - 325, 340 & 388 nm triplet + A-Band cloud pressure; 101 - 317, 340 & 388 nm triplet + climatological cloud pressure (A-Band cloud pressure file exists); 111 - 317, 340 & 388 nm triplet + climatological cloud pressure (A-Band cloud pressure file does not exist);

				<p>102 - 325, 340 & 388 nm triplet + climatological cloud pressure (A-Band cloud pressure file exists);</p> <p>112 - 325, 340 & 388 nm triplet + climatological cloud pressure (A-Band cloud pressure file does not exist).</p>
ErrorFlag	Integer*2	2048x2048	Unitless	<p>Error flag for retrieved total ozone column:</p> <p>1 - for column ozone outside of lookup table</p> <p>2 - for retrievals that did not converge due to bad measurements</p>
NValue	Real*4	4x2048x2048	N-value	Logarithm of measured albedo (Eq. 8) at 317 nm, 325 nm, 340 nm, and 388 nm. (soft calibrations included)
Residual	Real*4	3x2048x2048	N-value	Differences between measured and computed N-values with wavelength independent surface reflectivity (before the triplet algorithm) for channels 317 nm, 325 nm and 340 nm.
DNDOmega	Real*4	3x2048x2048	1/DU	$dN_x/d\Omega$, calculated ozone sensitivities of albedos at 317 nm, 325 nm and 340 nm.
DNDreflectivity	Real*4	4x2048x2048	N-Value/RU	dN_x/dR , calculated surface reflectivity sensitivities of albedos at 4 channels (317 nm, 325 nm, 340 nm, and 388 nm)
ColumnWeightFunctionPercent	U8LE	11x2048x2048	percent	Column Weighting Function (multiplied by 100) represent calculated sensitivity of retrieved total ozone column to ozone changes in each of 11 layers (from bottom to top).
YearDaySeconds	Integer*4	3	Unitless	Year, Day of year, Seconds in UTC
Wavelength	Real*4	4	nm	Centroids of filter bandpasses for 317 nm, 325 nm, 340 nm, and 388 nm
CalibrationCoef	Real*4	4	Counts/s* mW/m ² /nm	Calibration coefficients - multiplication factors that convert L1b raw count rates to the albedo for 317 nm, 325 nm, 340 nm, and 388 nm
NvalueAdjust	Real*4	4	N-Value	Soft-calibration adjustments to the logarithm of the albedo measurements at 317 nm, 325 nm, 340 nm, and 388 nm
NoABandCloud	Integer*4	1	Unitless	A flag set to 1 if EPIC cloud product file does not present for input.
RamanCorrection	Real*4	4x8	Percent	Raman inelastic scattering correction coefficients in percentage to radiance.
ControlFileContents	String	26	Unitless	Processing control file text dump

5. Version 3 Total Ozone: data quality and screening

The measurements from four EPIC UV channels are used to derive the global distributions of total ozone over the entire sunlit portion of the Earth. The core of the Version 3 ozone retrieval algorithm remained the same as in previous version 2 [Herman *et al.*, 2018], but several key modifications had been implemented aimed to improve total ozone retrievals. These modifications, described in details in Sec. 3, include: a) switch to Version 3 Level 1 product with improved geolocation registration, flat field and dark counts corrections; b) replace OMI based cloud height climatology with the simultaneous EPIC A-Band cloud height; c) update absolute calibrations using polar orbiting SNPP OMPS; d) add corrections for ozone profile shape and temperature; e) update algorithm and error flags to filter data; f) add column weighting functions for each observation to facilitate error analysis.

Comparisons of EPIC's total ozone with overlapping satellite instruments (SNPP OMPS and Aura OMI) demonstrated a good agreement with mean biases are mostly within ± 5 DU (or ± 1.5 -2%).

20 April 2020

hhmmss = 170725

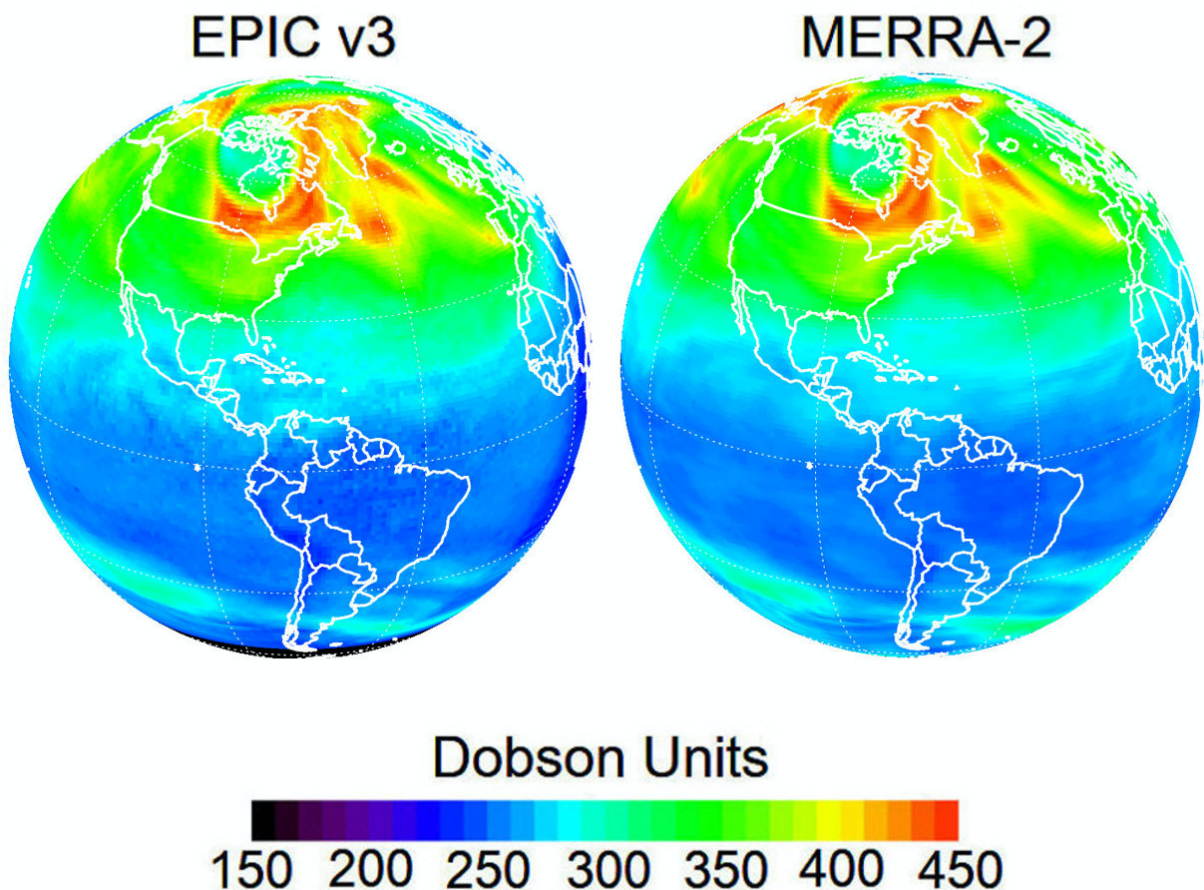


Figure 3. EPIC version 3 and MERRA-2 synoptic total ozone maps obtained on April 20, 2020 at around 17:05 UTC.

EPIC synoptic ozone maps are derived every 1-2 hours with multiple observations over the same location from sunrise to sunset each day. Figure 3 shows an EPIC synoptic total ozone map on April 20, 2020 along with a corresponding map from MERRA-2, which is an assimilated product that is based on Aura OMI total ozone and Aura MLS stratospheric ozone profile data [Gelaro *et al.*, 2017]. Good agreement between the two maps (Fig. 3) demonstrates that EPIC captures small scale changes in the ozone fields. Larger differences at the edge of the EPIC image correspond to observations at large SZA and SLA. Our analysis shows that differences start to increase when EPIC SZA and SLA exceed 70°. Larger biases at high SZA and SLA were also observed in the analysis of previous version 2 of EPIC ozone [Herman *et al.*, 2018]. Errors in geolocation assignments of the EPIC measurements, remaining uncertainties in CCD flat-field calibrations, and uncertainties in the radiative transfer simulations at high SZA and SLA contribute to observed biases at high SZA and SLA between EPIC and correlative measurements.

The use of real-time cloud-height information, derived from simultaneous EPIC A-Band measurements, allowed to decrease noise in Version 3 total ozone retrievals. Figure 4 below shows a synoptic map of reflectivity (left panel in Fig. 4) derived from EPIC 388 nm with a strong cyclone in the center of the image over the equatorial western Pacific. The middle plot in Fig. 4 shows total ozone map derived using climatological cloud heights. The artificial structures in the total ozone field are clearly seen at the location of the cyclone. However, when the ozone algorithm uses the real-time cloud height product derived from the EPIC A-band (right panel in Fig. 4) the artificial structures goes away.

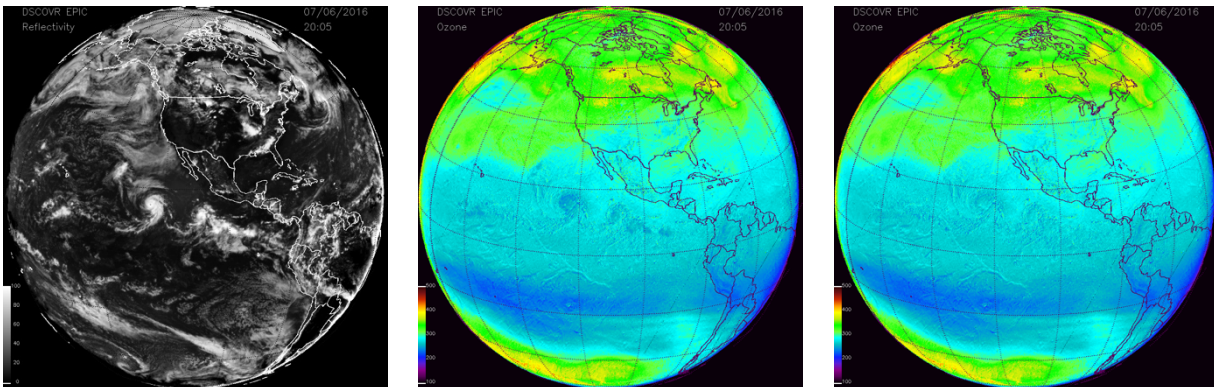


Figure 4. Synoptic maps of EPIC reflectivity (left) derived from 388 nm (in reflectivity units ranging from 0 to 1) and total ozone (in DU) derived using the OMI-based cloud height climatology (center) and real-time EPIC A-Band cloud height product (right) observed on July 6 2016 at 20:05 UTC..

EPIC Version 3 total ozone total columns had been evaluated using ozone observations from overlapping polar satellite instruments: Aura OMI and SNPP OMPS (see Fig. 5). In general, biases between EPIC and correlative satellite measurements are mostly within ± 5 DU (or ± 1.5 -2%). Biases are smaller in the tropics and increase at mid- and high latitudes, where biases tend to vary with the season, due to increasing SLA/SZA. The accuracy of the EPIC v3 has improved at high latitudes partially because of the use of the seasonal and latitude dependent a priori ozone/temperature profiles in TOA albedo calculations. EPIC v3 total ozone agreed with OMI and OMPS within $\pm 3\%$ with a better agreement in the Northern than in the Southern Hemisphere, due to profile sensitivity [Herman *et al.*, 2018].

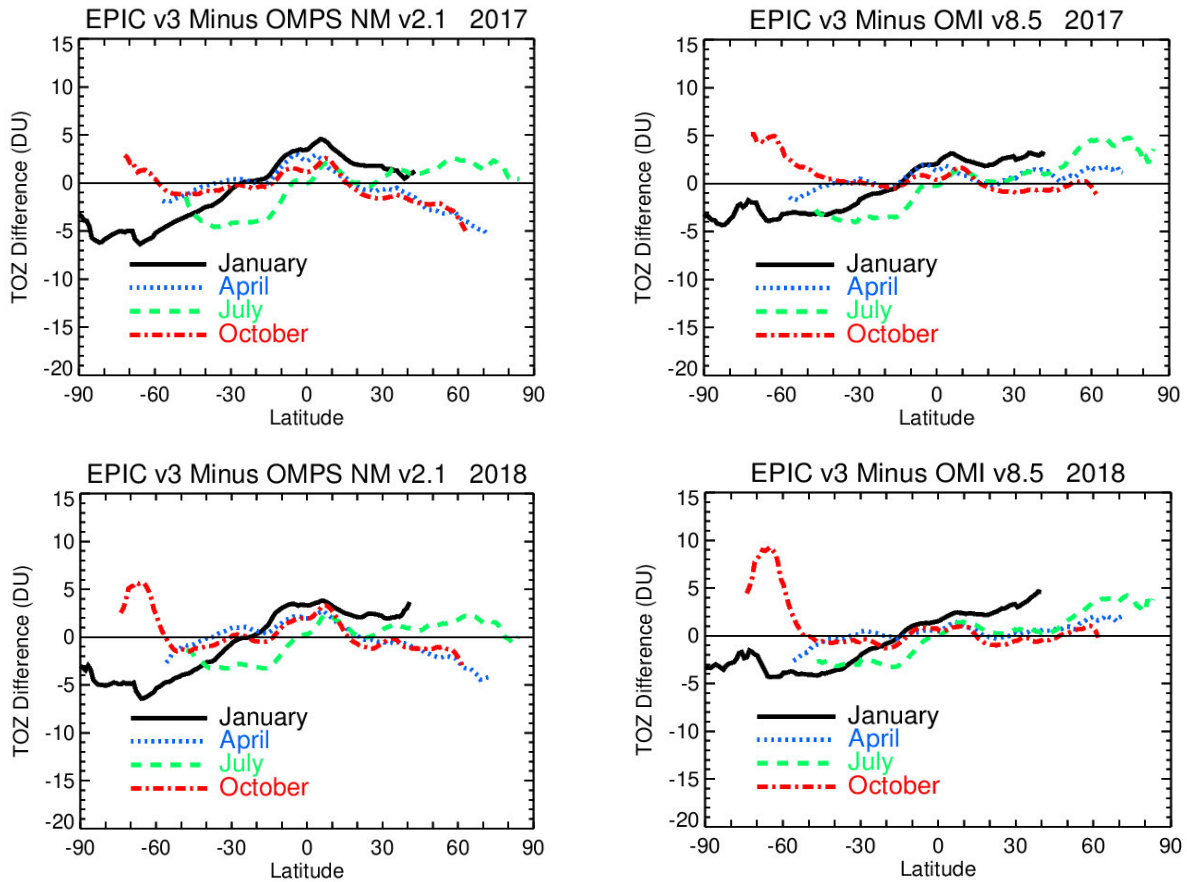


Figure 5. Mean seasonal biases in DU between EPIC version 3 and OMPS NM (left column) and Aura OMI (right column) in 2017 (upper row) and 2018 (lower row). Different colors correspond to different months. In general, biases between EPIC and overlapping satellite instruments are within ± 5 DU (or ± 1.5 -2%).

In addition, EPIC total ozone retrievals had been compared with ground-based observations. Figure 6 shows time series of total ozone columns in 2018 observed by EPIC (black lines) over 6 ground-based stations that measure total ozone using Brewer spectrometers (red lines). There is a high correlation between EPIC and Brewer measurements (>0.96) with mean biases ranging between -6 and 5 DU ($\sim 1.5\%$).

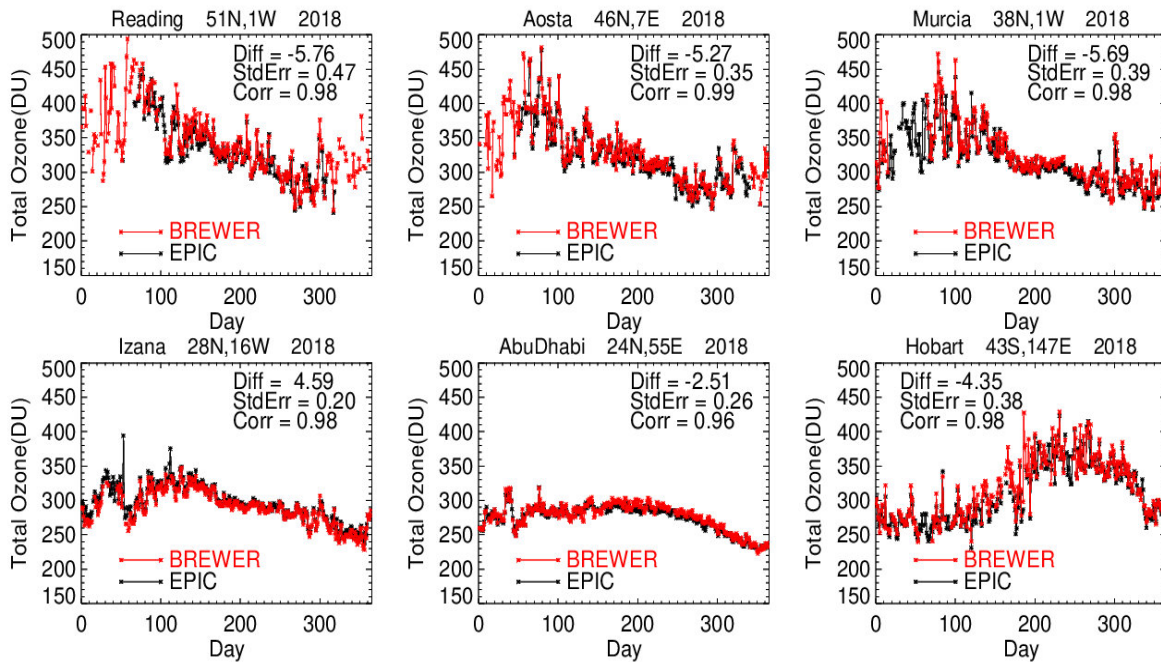


Figure 6. Time series of daily total column observations [DU] in 2018 at 6 different locations: Reading, Aosta, Murcia, Izana, Abu-Dhabi and Hobart. EPIC version 3 total ozone measurements are shown in black and ground-based Brewer observations are shown in red. Mean biases between EPIC and Brewer [DU], standard error of the mean [DU] and correlation are indicated for each location. Mean biases between EPIC and ground-based observations are ranging between -6 and 5 DU (or $\pm 1.5\%$).

For the comparisons shown in Figs. 5-6 EPIC’s total ozone values had been filtered limiting to observations with SZA and SLA less than 70° . Our analysis indicates that the quality of ozone retrievals from EPIC degrades as SZA and SLA exceeds $\sim 70^\circ$. Figure 7 shows total ozone observations at equatorial latitudes (20°S - 20°N) on July 11, 2020 as a function of SZA (top) and SLA (bottom). Total ozone does not vary significantly in the tropics. However, the plots in Fig. 7 show a systematic change in retrieved ozone as SZA and SLA exceed 70° . It is also obvious that ozone retrievals derived from two triplets 317.5 and 325 nm do not agree with each other for SZA/SLA 60 - 70° . The 325 nm triplet is typically used at high optical depth when SZA and SLA are quite large. This problem with systematic biases in EPIC total ozone retrievals at high SZA and SLA had been noted before in validation of version 2 EPIC data [Herman et al., 2018]. Several factors contribute into increased biases at high SZA and SLA, including remaining errors in geolocation assignments of the EPIC measurements, CCD flat-field calibrations, absolute calibrations, and uncertainties in the radiative transfer simulations at high SZA and SLA.

Therefore, for scientific applications of EPIC version 3 total ozone data we recommend the following data screening approach: a) use EPIC retrievals with SLA or SZA less than 70° , and b) use only pixels with Error Flag equal 0 and Algorithm Flag equal to 1, 101 or 111 (corresponds to 317.5 nm triplet).

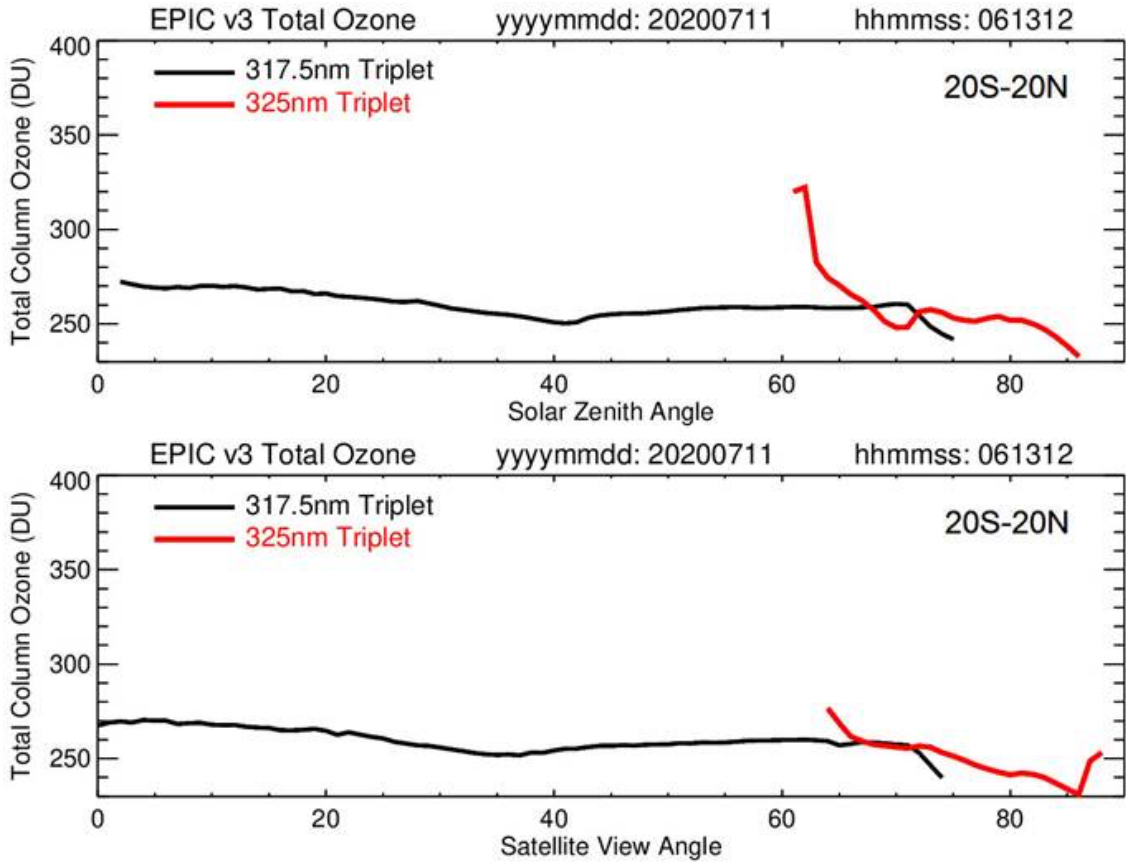


Figure 7. EPIC version 3 total column observations [DU] on July 11 2020 in equatorial latitudes (20S-20N) as a function of SZA (top) and SLA (bottom). EPIC retrievals with 317.5 nm triplet are shown in black and 325 nm triplet in red. Total ozone variability is expected to be very small in the tropics. Systematic errors in EPIC measurements are responsible for changes in retrieved total ozone at high SZA and SLA. For scientific analysis, we recommend to use EPIC total ozone retrievals from 317.5 nm triplet (algorithm flag equal 1, or 101, or 111) and limit SZA and SLA to less than 70°.

References:

- Bhartia, P. K., and C. W. Wellemeyer, "OMI TOMS-V8 Total O₃ Algorithm", Algorithm Theoretical Baseline Document: OMI Ozone Products, P. K. Bhartia (ed.), vol. II, ATBD-OMI-02, version 2.0, Aug. 2002.
- Bhartia, P. K., R. D. McPeters, L. E. Flynn, et al. 2013. "Solar Backscatter UV (SBUV) total ozone and profile algorithm." *Atmos. Meas. Tech.* 6 (10): 2533-2548 [10.5194/amt-6-2533-2013]
- Brion, J., Chakir, A., Charbonnier, J., Daumont, D., Parisse, C., and Malicet, J.: Absorption spectra measurements for the ozone molecule in the 350–830 nm region, *J. Atmos. Chem.*, 30, 291–299, 1998.
- Caudill, T. R., Flittner, D. E., Herman, B. M., Torres, O., and McPeters, R. D.: Evaluation of the pseudo-spherical approximation for backscattered ultraviolet radiances and ozone retrieval, *J. Geophys. Res.-Atmos.*, 102, 3881–3890, 1997.
- Daumont, D., Brion, J., Charbonnier, J., and Malicet, J.: Ozone UV spectroscopy I: Absorption cross-sections at room temperature, *J. Atmos. Chem.*, 15, 145–155, 1992.
- Dobber, M., Voors, R., Dirksen, R., Kleipool, Q., and Levelt, P.: The high resolution solar reference spectrum between 250 and 550 nm and its application to measurements with the Ozone Monitoring Instrument, *Sol. Phys.*, 249, 281–291, 2008.
- Herman, J., Huang, L., McPeters, R., Ziemke, J., Cede, A., and Blank, K.: Synoptic ozone, cloud reflectivity, and erythemal irradiance from sunrise to sunset for the whole earth as viewed by the DSCOVR spacecraft from the earth–sun Lagrange 1 orbit, *Atmos. Meas. Tech.*, 11, 177-194, <https://doi.org/10.5194/amt-11-177-2018>, 2018.
- Seftor, C. J., G. R. Jaross, M. E. Kowitt, et al. 2014. "Postlaunch performance of the Suomi National Polar-orbiting Partnership Ozone Mapping and Profiler Suite (OMPS) nadir sensors." *J. Geophys. Res. Atmos.* 119 (7): 4413-4428 [10.1002/2013JD020472]
- Joiner, J., and P. K. Bhartia, The determination of cloud pressures from rotational Raman scattering in satellite backscatter ultraviolet measurements, *J. Geophys. Res.*, 100(D11), 23019-23026, doi:10.1029/95JD02675, 1995.
- Kleipool, Q.L., Dobber, M.R., de Haan, J.F., and Levelt, P. F., Earth surface reflectance climatology from 3 years of OMI data, *J. of Geophys. Res.* 113, D18308, doi:10.1029/2008JD010290, 2008
- Klenk, K. F., P. K. Bhartia, E. Hilsenrath, and A. J. Fleig, "Standard Ozone Profiles From Balloon and Satellite Data Sets," *J. Climate Appl. Meteorol.*, 22, 2012–2022, 1983.
- Malicet, J., Daumont, D., Charbonnier, J., Chakir, C., Parisse, A., and Brion, J.: Ozone UV Spectroscopy II: Absorption cross sections and temperature dependence, *J. Atmos. Chem.*, 21, 263–273, 1995.
- Richard D. McPeters, P. K. Bhartia, Arlin J. Krueger, and Jay R. Herman, *Nimbus–7 Total Ozone Mapping Spectrometer (TOMS) Data Products User's Guide*, NASA/Goddard Space Flight Center Greenbelt, MD 20771, 1996.
- McPeters, R., G. Labow, and J. Logan. 2007. "Ozone climatological profiles for satellite retrieval algorithms." *J Geophys Res* 112 D05308
- McPeters, R. D., S. M. Frith, N. A. Kramarova, J. R. Ziemke, and G. J. Labow, *Trend Quality Ozone from NPP OMPS: the Version 2 Processing*, *Atmos. Meas. Tech.*, in review, 2018.
- Rodgers, C. D.: *Inverse methods for atmospheric sounding, Theory and Practice; Series on Atmospheric, Oceanic and Planetary Physics, vol.2*, World Scientific, 2000.

Rodriguez, J. V., Seftor, C. J., Wellemeyer, C. G., and Chance, K.: An overview of the nadir sensor and algorithms for the NPOESS ozone mapping and profiler suite (OMPS), *Proc. SPIE 4891, Optical Remote Sensing of the Atmosphere and Clouds III*, 65 (9 April 2003), <https://doi.org/10.1117/12.467525>, 2003.

Vasilkov, A., J. Joiner, R. Spurr, P. K. Bhartia, P. Levelt, and G. Stephens, Evaluation of the OMI cloud pressures derived from rotational Raman scattering by comparisons with other satellite data and radiative transfer simulations, *J. Geophys. Res.*, 113, D15S19, doi:10.1029/2007JD008689, 2008.

Yang, Y., Meyer, K., Wind, G., Zhou, Y., Marshak, A., Steven Platnick, S., Min, Q., Davis, A., Joiner, J., Vasilkov, A., Duda, D., and Su, W., Cloud products from the Earth Polychromatic Imaging Camera (EPIC): algorithms and initial evaluation, *Atmos. Meas. Tech.*, 12, 2019–2031, 2019